International Journal of Recent Advances in Multidisciplinary Topics Volume 6, Issue 10, October 2025

www.ijramt.com | E-ISSN: 2582-7839 | RESAIM Publishing (www.resaim.com)

Optimal Tuning of Fractional Order Sliding Mode Controller with Adaptive CS Algorithm for PMSM Speed Control

Kum Song Choe¹, Tong Chol Kim^{2*}

1.2 Faculty of Automation Engineering, Kim Chaek University of Technology, Pyongyang, Democratic People's Republic of Korea

Abstract: To improve dynamic quality and control performance of permanent magnet synchronous motor (PMSM) speed control, the fractional order sliding mode controller (FOSMC-PID) with PID sliding surface was designed and its parameters were tuned optimally by adaptive Cuckoo Search (CS) algorithm. The newly proposed adaptive rules of the Lévy distribution and abandon probability coefficients in adaptive CS algorithm ensure the optimal tuning of the controller parameters. The proposed control system achieves small chattering phenomenon with fast convergence speed in PMSM speed control. Through MATLAB simulation, the PMSM speed control performance of integer-order SMC and fractional-order SMC, and the parameter tuning results by CS algorithm and PSO algorithm are compared and analyzed. The simulation results show that the proposed controller design method not only has good dynamic response but also has strong robustness to disturbances.

Keywords: Cuckoo Search Algorithm (CSA), Fractional Order Sliding Mode Controller (FOSMC), Optimal Tuning, PMSM Speed Control.

1. Introduction

Permanent magnet synchronous motors (PMSM) have been widely applied in industry due to their excellent characteristics such as high efficiency, high power density and high torque-toinertia ratio. However, the practical PMSM system is a typical nonlinear multivariable coupling system so which is sensitive to unmodeled dynamics, parameter variations and load disturbances. To improve the dynamic performance of PMSM systems, various robust control approaches have been adopted, such as adaptive control, [1], [2] intelligent control, [3] SMC, [4]-[6] adaptive disturbance rejection control (ADRC), [7] etc. SMC has been widely applied to PMSM control due to plant variations, parameter disturbances, simplicity implementation, and strong robustness.

SMC is a branch of variable structure systems (VSS). The basic idea of sliding mode control is to control a complex higher-order system by referring to a single state variable, i.e., a sliding function. The most important feature of sliding mode control (SMC) is its fast convergence and simplicity in practical applications. Also, it has been widely used for nonlinear system control due to its high robustness to external disturbances, modeling errors and insensitivity to changes in plant

parameters. SMC has been applied in many fields such as PMSM, [4], [5], [8] induction motor, [9] brushless DC motor, [10] power conversion system, [11] etc., and has also been studied. The theoretical study of SMC mainly focused on overcoming two critical drawbacks. That is, the oscillations of the control action and the unknown behavior in the reaching state. The oscillation phenomenon of the control action is usually reduced by approximating the signal function to a saturation function. The unknown behavior in the reaching process ensures the robustness of the system by introducing a dynamic sliding surface. Wu and Yu [12] designed terminal SMC to achieve fast convergence and high accuracy in sliding state. Xinghuo, [13] Mu [14] and Lu [15] introduced NTSMC, NFTSMC, which can solve the singularity problem with initial conditions. Also, Huang [16] and Bigdeli [17] have achieved better control performance by designing fractional SMC for complex nonlinear systems and chaotic systems represented in fractional form. Theoretically, fractional order sliding surfaces undergo slower energy transfer during switching, and thus produce smaller chattering compared to integer order sliding surfaces that decrease exponentially to zero. Zaihidee, [18] Huang [19] and Abdelhamid [20] have experimentally demonstrated that fractional-order SMC has better control performance with smaller chattering and robustness against external load disturbance and parameter variations compared to integer-order SMC.

Recently, a combination of SMC and artificial intelligence has been achieved to achieve better control performance. Using intelligent optimization algorithms, the structure and parameters of SMC controllers are tuned online or offline to maximize the performance of SMC. Mahmoodadi [21] applied an adaptive genetic algorithm consisting of new crossover and mutation operators to control sliding, solving the low convergence rate and local optimization problem. Laware [22] achieved high performance by tuning SMC parameters using non-dominated sorting genetic algorithm II (NSGA-II) and multi-objective particle swarm optimization (MOPSO). The switching gain of the sliding controller is optimized by PSO algorithm and its effectiveness in UAV and intelligent vehicle control is verified [23]-[27]. Terfia et al. [28] tuned three

sliding switching gains using a grey wolf optimization algorithm, and Lindokuhle et al. [29] compared the performance of four SMC parameters tuning by the ant colony optimization algorithm to GA.

Anuja [30] has shown good results by comparing and evaluating the performance of heuristic optimization algorithms, PSO, GA and ACO, in the application field of the Cuckoo Search Algorithm (COA) and the optimal search. The cuckoo search algorithm, developed by Xin-She Yang and Suash Deb in 2009, has many applications in optimization problems due to its excellent global optimization performance [30]. This algorithm is a natural-based heuristic algorithm that mimics Lévy flight random walk and the special breeding and oviposition mechanism of some cuckoos. Adult cuckoo lays eggs in the nests of other birds, which are found in host birds and are not removed, and then it grows and matures. Due to the migratory and environmental characteristics of these cuckoo populations, during the breeding process, the population reaches a solution (nest) where the objective function is optimal [30]. Cuong-Le et al. [32] applied the CS algorithm to various nonlinear multi-objective optimization problems and showed good solution results. Zamani et al. [31] showed good disturbance rejection performance and robustness by tuning the parameters of fractional-order PID controller with the cuckoo search algorithm.

In this paper, we propose a new adaptive formulation of variable step coefficient β and abandon probability p_a , and optimally tune the controller parameters of FOSMC for PMSM speed control, to verify its effectiveness through simulation. The rest of the paper is organized as follows. In Section 2, the fractional calculus and approximation implementation for fractional order operations are introduced. In Section 3, based on the mathematical modeling of PMSM, a fractional order sliding controller with PID sliding surface is designed and analyzed for stability. Section 4 describes the newly proposed adaptive cuckoo search algorithm. In Section 5, we compare integer-order SMC and fractional-order SMC through MATLB simulation, and compare and discuss the tuning results by CS and PSO algorithms. Section 6 concludes the work and discusses future research directions.

2. Fractional Calculus and Approximation

The fractional order operation generalizes the integrand of integer order to the non-integer calculus. The basic operator $_{a}D_{t}^{\alpha}$ is defined as follows.

$$D^{\alpha} = {}^{\Delta}_{a} D^{\alpha}_{t} = \begin{cases} \frac{d^{\alpha}}{dt^{\alpha}}, & \alpha > 0\\ 1, & \alpha = 0\\ \int_{a}^{t} (d\tau)^{-\alpha}, & \alpha < 0 \end{cases}$$
 (1)

where a and t denote the upper and lower intervals and $\alpha \in \Re$ denotes the degree.

We use the Riemann-Liouville (RL) definition which introduces the gamma function $\Gamma(\cdot)$.

$${}_{a}D_{t}^{\alpha}f(t) = \frac{1}{\Gamma(n-\alpha)} \frac{d^{n}}{dt^{n}} \int_{a}^{t} \frac{f(\tau)}{(t-\tau)^{\alpha-n+1}} d\tau$$

$$n-1 \le \alpha < n$$
(2)

The Laplace transform of fractional differential based on the RL definition is as follows:

$$\int_0^\infty {_0D_t^\alpha f(t)e^{-st}dt} = s^\alpha L\{f(t)\} - \sum_{k=0}^{n-1} s^k {_0D_t^{\alpha-k-1}f(t)}|_{t=0}$$
 (3)

where $L\{\cdot\}$ means Laplace operator.

The fractional order operation is implemented using the Oustaloup approximation.

$$s^{\alpha} \approx K \prod_{n=-N}^{N} \frac{1 + \left(\frac{s}{\omega_{z,n}}\right)}{1 + \left(\frac{s}{\omega_{p,n}}\right)}, \quad \alpha > 0$$
 (4)

where 2N+1 means the number of zeros and K means the gain that makes the above equation have a unity gain at 1 rad/s

 $\omega_{z,n}, \omega_{p,n}$ is defined as follows;

$$\omega_{z,n} = \omega_b \left(\frac{\omega_h}{\omega_b}\right)^{(n+N+(1-\alpha)/2)/(2N+1)}$$
(5)

$$\omega_{p,n} = \omega_b \left(\frac{\omega_h}{\omega_b}\right)^{(n+N+(1+\alpha)/2)/(2N+1)}$$
(6)

where ω_h, ω_h is the upper and lower bounds of the approximation interval and satisfies $\omega_h \omega_h = 1, k = \omega_h^{\alpha}$.

3. Fractional-Order Sliding Mode Controller (FOSMC) **Design for PMSM Speed Control**

A. Mathematical Model of PMSM

The PMSM consists of a stator and a rotor, which is made of a permanent magnet, and the stator has a sinusoidally separated three-phase winding.

To obtain the model of PMSM, the following assumptions are made for the plant [5]. There is no damp winding in the rotor, neglecting eddy current, hysteresis losses, magnetic saturation, and assuming that the induced EMF is sinusoidal.

Under the above assumptions, the mathematical model of PMSM is as follows [7].

$$u_d = R_s i_d + \dot{\lambda}_d - \omega_e \lambda_q \tag{7}$$

$$u_q = R_s i_q + \dot{\lambda}_q + \omega_e \lambda_d \tag{8}$$

$$T_e = p_n \left[\psi_f i_q + (L_d - L_q) i_d i_q \right] \tag{9}$$

$$\omega_{e} = p_{n}\omega_{r} \tag{10}$$

where u_d , u_q are the d, q-axis stator voltages, respectively; i_d, i_q are the d, q-axis stator currents, respectively; L_d, L_q are the d, q-axis stator inductances, respectively; T_e is the electric torque; p_n is the pole pair; ω_e is the electrical angular velocity and ω_r is the rotor speed. ψ_f is the flux linkage of the permanent magnet.

For surface PMSM, we have $L_d = L_a$; thus, the electromagnetic torque equation is rewritten as follows:

$$T_e = p_n \psi_f i_a = k_t i_a \tag{11}$$

where k_t is defined as follows:

$$k_t = p_n \psi_f \tag{12}$$

The mechanical dynamic equation is as follows:

$$T_{\rho} = J\dot{\omega}_r + B_m \omega_r + T_L + d(t) \tag{13}$$

$$\dot{\omega}_r = \frac{1}{I} \left(k_t i_q - B_m \omega_r - T_L - d(t) \right) \tag{14}$$

where J is the motor moment inertia constant, B_m is the viscous friction coefficient, T_L is the external load torque and $|d(t)| \le D$ is the bounded disturbance.

In this paper, the main control objective is to asymptotically track the motor speed ω_r to the desired speed ω_r^* . To achieve the control object, a sliding mode controller is designed that provides the set-point value of the stator q-axis current controller in the speed control loop. Then, for decoupling control, the i_d is set to 0.

The speed tracking error e(t) and its derivative are defined as follows:

$$e(t) = \omega_r^*(t) - \omega_r(t) \tag{15}$$

$$\dot{e}(t) = \dot{\omega}_r^*(t) - \dot{\omega}_r(t) = \dot{\omega}_r^*(t) - \frac{1}{I} \left(k_t i_q - B_m \omega_r - T_L \right)$$
 (16)

B. Fractional Order Sliding Mode Controller (FOSMC) Design

First, the fractional-order PID ($PI^{\alpha}D^{\beta}$) sliding surface is designed as follows:

$$S(t) = k_p e(t) + k_i D^{-\alpha} e(t) + k_d D^{\beta} e(t)$$

$$k_p, k_i, k_d > 0, 0 < \alpha < 1, 0 < \beta < 1$$
(17)

where $D^{-\alpha}(\cdot)$ is α th-order fractional integral; $D^{\beta}(\cdot)$ is β th-order fractional differential.

$$\dot{S}(t) = k_n \dot{e}(t) + k_i D^{1-\alpha} e(t) + k_d D^{\beta+1} e(t)$$
(18)

Substituting Eq. (16) into Eq. (18), we have

$$\dot{S}(t) = k_p \dot{\omega}_r^*(t) - \frac{k_p}{J} \left(k_t i_q - B_m \omega_r - T_L - d(t) \right) + k_i D^{1-\alpha} e(t) + k_d D^{\beta+1} e(t)$$
(19)

Above Eq. (19), disturbance term set d(t) = 0, forcing $\dot{S}(t) = 0$ and then the equivalent control u_{eq} can be obtained

$$u_{eq} = i_q^{eq} = \frac{J}{k_p k_t} \left(k_p \dot{\omega}_r^*(t) + \frac{k_p}{J} \left(B_m \omega_r + T_L \right) + k_i D^{1-\alpha} e(t) + k_d D^{\beta+1} e(t) \right)$$
(20)

To reduce the chattering problem, the sign function is substituted by the following function:

$$sat(S(t)) = \frac{S(t)}{|S(t)| + \varepsilon}$$
(21)

where ε is sufficiently small positive constant.

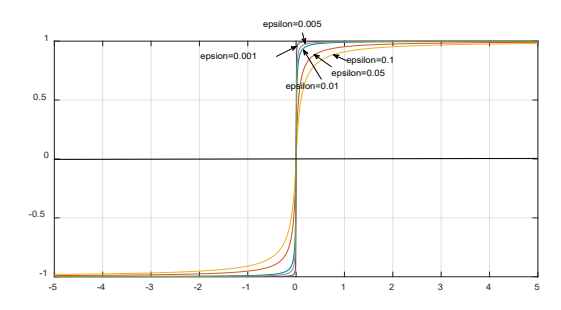
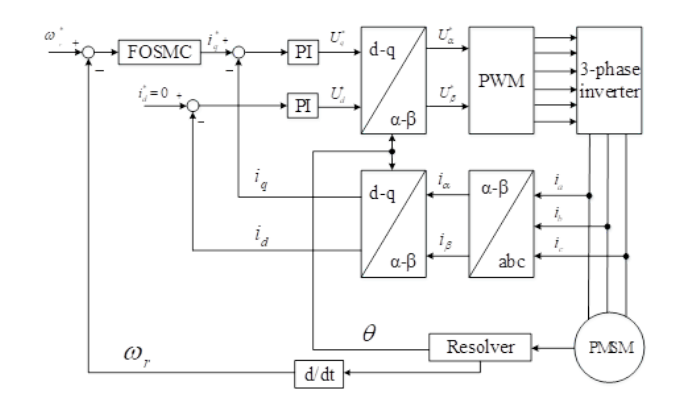


Fig. 1. sat(S(t)) function curve with ε

As shown in Fig. 1, with increasing ε , the saturation function near zero becomes smooth and the effect of vibration is reduced. However, if ε is too large, the amplitude will increase and the sliding motion time will be longer, so that ε should be chosen properly.

Based on the design of fractional order sliding controller, the PMSM speed control system is constructed as shown in Fig. 2.



fast rate.

Fig. 2. PMSM speed control system diagram with FOSMC

$$u = i_{q}^{*} = u_{eq} + k_{S} sat(S(t)) =$$

$$= \frac{J}{k_{p} k_{t}} \left(k_{p} \dot{\omega}_{r}^{*}(t) + \frac{k_{p}}{J} \left(B_{m} \omega_{r} + T_{L} \right) + k_{i} D^{1-\alpha} e(t) \right) + k_{d} D^{\beta+1} e(t) + k_{S} \frac{S(t)}{|S(t)| + \varepsilon}$$
(22)

As can be seen in Fig. 2, the output of fractional order sliding controller is the set point of PI controller of q-axis current regulation loop.

C. Stability Analysis

The Lyapunov function is defined as follows:

$$V = \frac{1}{2}S^2(t) \tag{23}$$

According to the Lyapunov stability theorem, the sliding surface reaching condition is $S(t)\dot{S}(t) < 0$.

Using the result obtained by substituting Eq. (19) into Eq. (22) for the derivation of the above expression, we have,

$$\dot{V} = S(t)\dot{S}(t) = \frac{k_p}{J}S(t)\left(\frac{d(t)}{k_t} - k_S \frac{S(t)}{|S(t)| + \varepsilon}\right)$$
(24)

To become S(t)S(t) < 0, k_s must satisfy bellow equation;

$$k_s > \frac{d(t)}{k_t} \frac{S(t) + \varepsilon}{S(t)} \tag{25}$$

1) When
$$S(t) < 0$$
 then $\frac{S(t)}{|S(t)| + \varepsilon} < 0$,

$$\left(\frac{d(t)}{k_t} - k_S \frac{S(t)}{|S(t)| + \varepsilon}\right) > 0 \Rightarrow S(t)\dot{S}(t) < 0 \tag{26}$$

2) When $\varepsilon < S(t)$

$$k_{s} = 2\frac{d(t)}{k_{t}} > \frac{d(t)}{k_{t}} \frac{S(t) + \varepsilon}{S(t)} \Rightarrow$$

$$k_{s} = 2\frac{d(t)}{k_{t}} > \frac{d(t)}{k_{t}} \frac{S(t) + \varepsilon}{S(t)} \Rightarrow (27)$$

3) For the properly large positive number M, when $0 < S(t) \le \varepsilon$

$$k_s = M \frac{d(t)}{k_t} > \frac{d(t)}{k_t} \frac{S(t) + \varepsilon}{S(t)}$$
(28)

1. when
$$S(t) \le \varepsilon$$
, i.e, if $\frac{S(t) + \varepsilon}{S(t)} \le M$, then $\dot{S}(t) < 0$,

and Eq. (27) holds and the system is stable.

- 2. when $0 < S(t) << \varepsilon$, i.e., if $\frac{S(t) + \varepsilon}{S(t)} > M$, $\dot{S}(t) >> 0$, and the system is unstable. On the other hand, S(t) is stable by moving to the 1 state at a very
- 3. After several oscillations and controls, passing between stages 1 and 2, the sliding surface S(t) is finally maintained at $S(t) = \varepsilon/(M-1)$, then becomes $\dot{S}(t) = 0$, and the system reaches a steady state.

Through the above analysis, if we choose M, ε properly such that Eq. (28) is satisfied, and obtain the switching gain k_s , the system will converge to zero in a finite time.

4. Optimal Tuning of Fractional Order Sliding Mode Controller using Adaptive CS algorithm

A. Lévy Flight

In general, animals are found to feed in a random or quasirandom manner.

The foraging path of animals is a random walk, because the next move is based on the transition probability to the next position or state in the current position or state. The transition probabilities are clearly modeled mathematically and previous studies have shown that the flight behavior of many animals and insects is typical of Lévy flight.

The basic equation of Lévy flight is as follows [32].

$$L\acute{e}vy (\beta) = \frac{\sigma(\beta) \times u}{|V|^{1/\beta}}$$
 (29)

where u and V are drawn from normal distributions, i.e. $u \sim N(0, \sigma_u^2), \ V \sim N(0, \sigma_v^2),$ and the parameter $1 < \beta \le 2$ is considered to control the range of the step lengths.

Where σ_u , σ_v are expressed as follows:

$$\sigma_{u} = \left\{ \frac{\Gamma(1+\beta) \times \sin(\frac{\pi\beta}{2})}{\Gamma\left[\frac{(1+\beta)}{2}\right] \times \beta 2^{\left(\frac{\beta-1}{2}\right)}} \right\}^{\frac{1}{\beta}}, \sigma_{v} = 1$$
(30)

Here Gamma function is denoted integral as follows:

$$\Gamma(z) = \int_{0}^{\infty} t^{z-1} e^{-t} dt \tag{31}$$

The Lévy flight represents a random trajectory, and its step length is obtained according to the Lévy distribution as follows:

$$L\acute{e}vy \sim u = t^{-\beta}, (1 < \beta \le 2) \tag{32}$$

This means infinite variance with infinite mean.

B. Cuckoo Search Algorithm (CSA)

1) Cuckoo Search Rule

Generally, the cuckoo search is done with the following rules.

First, cuckoos lay one egg at a time and lay their eggs in the nest of a randomly selected host bird. Next, the best nest with good quality eggs is inherited in the next generation. Also, among nests, a probability $p_a \in [0,1]$ is found by the host bird, which either abandons the eggs or the nests and builds a new nest. That is, among n solutions, we replace the new solution by the p_a part.

2) Adaptive CS Algorithm

The cuckoo search algorithm can be divided into three main steps.

The first stage generates the initial solution, the second stage updates the solution with a Lévy random walk, and the third stage updates the new solution with a certain probability $P_a \in [0,1]$ of updating solutions.

The second and third steps above are repeated until they meet the specified number of iterations or search stopping condition.

In this study, the size of β adjusting the size of the Lévy random walk is adaptively varied as Eq. (34) to find the optimal one.

The larger the value between 1 and 2, the higher the probability that the length of the random walk will be reduced.

Therefore, the larger the number of iterations, the higher the probability of reaching the optimum point, the smaller the step size, and the search for the optimal solution is necessary. Also, the probability $P_a \in [0,1]$ affecting global optimization performance is varied as Eq. (36), which reduces the computational load without affecting global optimization performance.

Step 1: Generate N candidates initial solutions, set the number of maximum iterations T_{max}

For i=1:N

- Chose the initial solution of X_i (i = 1, 2, ..., N), N: Number of host nest
- 2. Evaluate the objective function: $f(X_i)$

Repeat Step 2 and Step 3 until $t < T_{\text{max}}$

Step 2: Find and update nest

3. for i=1:N

$$X_i^t = X_i^{t-1} + \alpha \oplus L\acute{e}vy^{(\beta)}$$
 (33)

where $\alpha \in rand(0,1)$ is chosen randomly each iterations

$$\beta = 1 + \sin\left(\frac{\pi t}{2T_{\text{max}}}\right), \qquad 1 < \beta \le 2 \tag{34}$$

Limit X_i^t in the boundaries condition $X_{\min} \le X_i^t \le X_{\max}$

- 4. Evaluate the fitness function of new solution $f_{obi}(X_i^t)$
- 5. If $f_{obj}(X_i^t) < f_{obj}(X_i^{t-1})$

update the new nest $X_i = X_i^t$

End if

End for

6. Rank the best fitness function and find the best

$$f_{best}^t = \min(\{f_{obj}(X_1^t), ..., f_{obj}(X_N^t)\})$$

Step 3: Host bird's decision-making process based on abandon fraction $P_a \in [0,1]$ with adaptive rule

7. Adaptive rule of abandon fraction P_a

$$\gamma_t = \gamma_{(t-1)} \times \frac{f_{best}^t}{f_{best}^{t-1}}$$
(35)

Where $\gamma_1 = 0.3$

$$P_a = 0.2 + \gamma_t \times \frac{T_{\text{max}} - t}{T_{\text{max}}} \tag{36}$$

8. Calculate the number of dumping nests: P_{nest}

$$P_{nest} = [P_a \times N] + 1 \tag{37}$$

9. Random selection of the dumping nest except for the best solution.

$$n = randsample([2:N], P_{nest})$$
(38)

- 10. For j=1:Pnest
- 11. Randomly choose $Temp_i^t$ in the solution intervals $(X_{\min} \leq Temp_i^t \leq X_{\max})$
- 12. Evaluate the fitness function of new solution $f_{obj}(Temp_j^t)$

13. If
$$f_{obj}(Temp_j^t) < f_{obj}(X_{n(j)}^t)$$

$$X_{n(j)}^t = Temp_j^t, \ f_{obj}(X_{n(j)}^t) = f_{obj}(Temp_j^t)$$

End if

End for

- 14. Rank the best fitness function and find the best solution
- 15. t = t + 1

5. Simulations and Results

The designed controller is simulated in MATLAB/Simulink environment and the speed control system is evaluated.

The model used in the simulation is a 3-phase PMSM of 1.93 kW and the parameters are shown in Table 1.

Table 1

Parameters of PMSM							
Parameter	Value						
Stator resistance, R_s	1.2Ω						
d-axis stator inductance, L_d	6.35mH						
Moment of inertia, J	$2.31\times10^{-4}kg\cdot m^2$						
Viscous friction coefficient, B_m	0.0002Nms						
Flux linkage, ψ_f	0.15 <i>Wb</i>						
Pole pair, p_n	4						
Load Torque, T_L	2.5N						

The control system designed in Simulink environment is

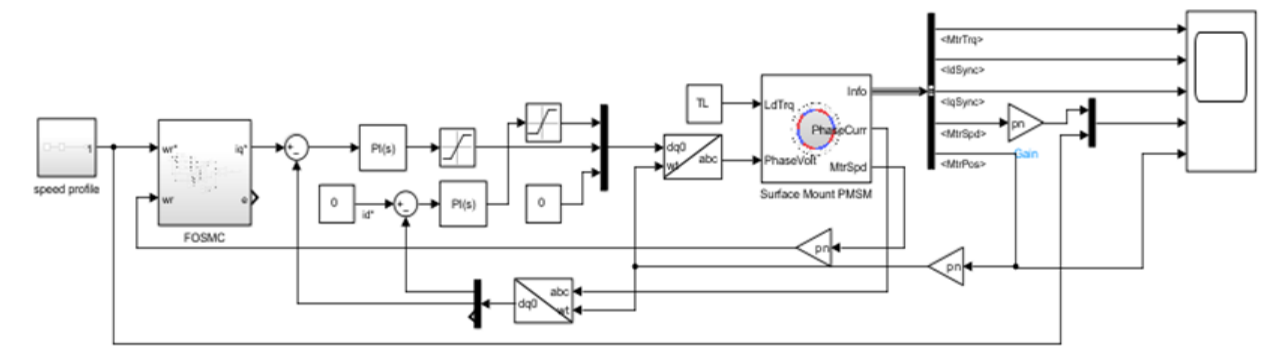


Fig. 3. Simulink diagram for PMSM speed control with fractional order sliding controller

constructed as shown in Figure 3.

In the simulation, we used the SPMSM model provided by MATLAB/Simulink. In the simulation, the control volume limit is given for each set point. We perform the adaptive CS algorithm operation on m-files and perform the simulation by setting the obtained solutions to the controller parameters.

The PI controller parameters of the current regulation loop are simulated by setting $k_{p_d} = 0.5$, $k_{i_d} = 200$, $k_{p_q} = 0.6$, $k_{i-q} = 250$. Also, the saturation function (Eq. 21) is set to $\varepsilon = 0.5$, M = 3, the upper limit of load disturbance is set to 2.4 times the load torque and is simulated by using $k_s > 6$.

Then, in the cuckoo search algorithm, set the number of candidate solutions N = 30, the maximum number of steps $T_{\rm max} = 100$, and the controller parameters are searched in the following intervals,

$$0 < k_p \le 1, 0 < k_i \le 1, \ 0 < k_d \le 1, \ 0 < alpha \le 1, \ 0 < beta \le 1,$$

$$2 < k_s \le 15$$

To minimize the steady-state error, the fitness function is defined as follows;

$$J = ITAE + M + t_s (98\%) + 100E_{ss}$$

The speed response and load disturbance response of the designed controller are compared and analyzed by simulation.

For comparison, the results obtained by optimally tuning the parameters of SMC and FOSMC with the CS algorithm are shown in Fig. 4.

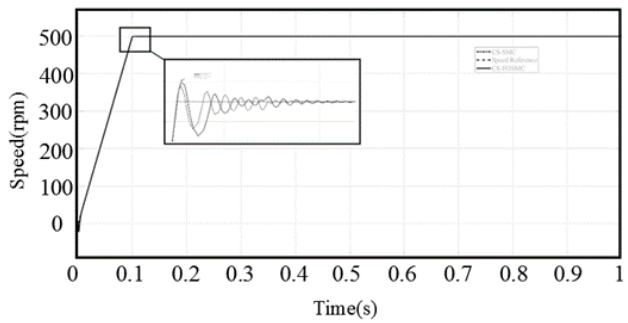


Fig. 4. Comparison tracking performance between FOSMC and Integer order

As shown in Fig. 4, FOSMC has a 0.3% less overshoot, 30% less chattering amplitude and significantly faster convergence rate than integer-order SMC.

Figure 5 shows the load disturbance rejection characteristics of FOSMC.

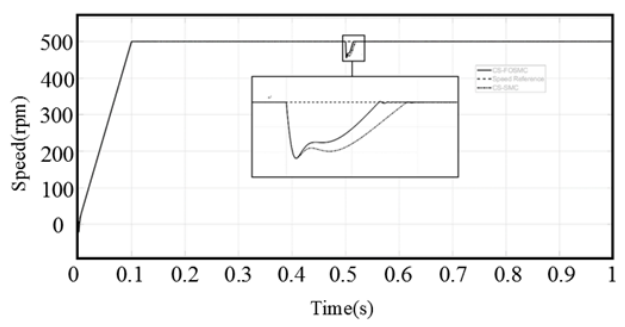


Fig. 5. Comparison disturbance suppression performance between FOSMC and Integer order SMC (6N step disturbance at 0.5s)

Initially, the disturbance rejection capability of 2.5 N load and 6 N load at 0.5 s was shown by comparison with integerorder SMC. As shown in the figure, the designed control system is stable and effectively suppressed even in external disturbances.

Next, the search performance of the proposed adaptive CS algorithm is compared with that of PSO algorithm.

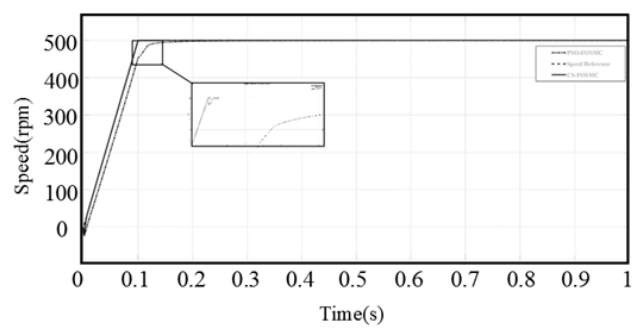


Fig. 6. Comparison speed response between Adaptive CS-FOSMC and PSO-FOSMC algorithm

The tracking and disturbance rejection performance between the FOSMC tuned with the adaptive CS algorithm and the PSO algorithm and the tuned FOSMC are shown in Fig. 6 and Fig. 7.

Table 2

Detailed control performance											
Algorithm	k_p	k_i	k_d	α	β	k_S	ITAE	M[%]	$t_S[s]$	E_{SS}	J
Adaptive CS	0.424	0.6364	0.6887	0.0167	0.0165	10.2298	0.0279	0.06	0.1	0.0221	2.3979
PSO	0.5553	0.7883	0.9419	0.0985	0.0905	13.2283	1.033	0.1	0.1	0.112	12.433

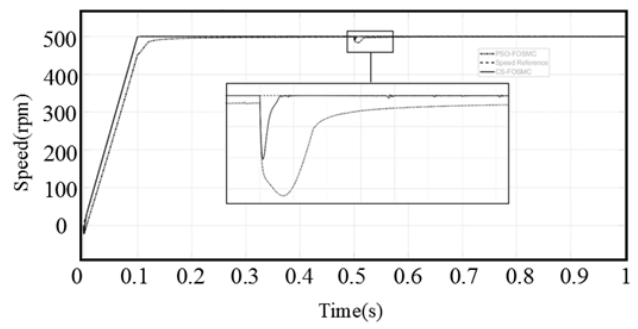


Fig. 7. Comparison disturbance suppression performance between CS FOSMC and PSO-FOSMC (6N step disturbance at 0.5s)

As shown in Fig. 6 and Fig.7, we can see that the search performance of the proposed adaptive CS algorithm is

It can be seen that the fitness function is optimized together with the control performance indices such as ITAE, steady-state error and overshoot.

The detailed control performance indices are shown in the table 2.

Figure 8 compares the search performance between the CS algorithm with adaptively varying discard probability and the CS algorithm with fixed discard probability.

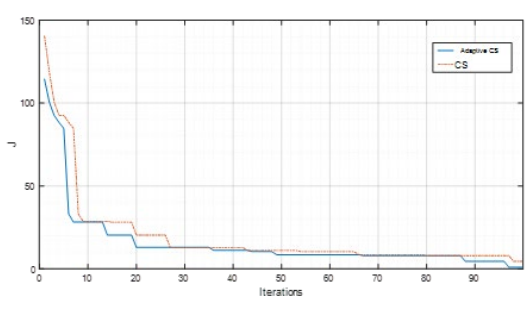


Fig. 8. Comparison performance between Adaptive CS and original CS

As shown in the figure, it can be seen that the adaptive CS algorithm can obtain a good solution with less iteration.

6. Conclusion

A systematic design method of fractional order sliding controller (FOSMC-PID) with fractional order PID sliding surface for PMSM speed control and an improved adaptive CS algorithm for optimal tuning of controller parameters are introduced.

By adjusting the controller parameters by taking the rise time, transient time, steady-state error, overshoot and ITAE parameters as objective functions, the excellent control performance and robust performance of the proposed controller are clearly shown. In addition, we have newly proposed a rule to adaptively change the Levy random walk length and abandon probability so as to increase the global search capability and search speed while reducing the computational effort.

The advantages of the proposed controller and algorithm are demonstrated through simulation. Although there is a lack of model uncertainties in the modeling process, the simulation shows good control performance under large load disturbances, which can suppress the model uncertainties from the strong robustness of the sliding controller.

In the future, we will study the application of the adaptive CS algorithm to multi-objective optimization of control systems in combination with fractional order control, neural network control, etc.

References

- Sabouni E, Merah B and Bousserhane I K. "Adaptive backstepping controller design based on neural network for PMSM speed control"; International Journal of Power Electronics and Drive Systems, 2021; 12(3): 1940-1952.
- Zhao S and Tan KK. Adaptive feedforward compensation of force ripples in linear motors. Control Engineering Practice 2018; 26(9):1081-1092.
- Fayez FM. "Intelligent optimal recurrent wavelet Elman neural network control system for permanent-magnet synchronous motor servo drive," IEEE Transactions on Industrial Informatics 2018; 14(4): 1986-2003.
- Wang YQ, Zhu YC, Feng YT, et al. New reaching law sliding mode control strategy for permanent magnet synchronous motor. Electric Power Automat Equip 2021; 41:192-198.
- Zaihidee FM, Mekhilef S, Mubin M. Robust Speed Control of PMSM Using Sliding Mode Control (SMC)-A Review. Energies 2019; 12:1669.
- Huang JC, Li HS, Chen YQ et al. Robust Position Control of PMSM Using Fractional-Order Sliding Mode Controller. Hindawi Publishing Corporation Abstract and Applied Analysis, Volume 2012; 1-33.
- Luo J, Wang LC, Liu BY. Low-speed control of PMSM based on ADRC + FOPID. Systems Science & Control Engineering 2021; 9(1): 73-87.
- Yu YJ, Zhu LH, Zhou F, et al. SPMSM speed sensorless control based on fuzzy sliding mode and new expanded state observer. Electr Mach Control 2021; 26: 1-16.
- Rong-Jong, W.; Kun-Lun, C.; Jeng-Dao, L. On-Line Supervisory Control Design for Maglev Transportation System via Total Sliding-Mode Approach and Particle Swarm Optimization. IEEE Trans. Autom. Control 2020, 65, 1544-1559.
- [10] Yaonan, W.; Xizheng, Z.; Xiaofang, Y.; Guorong, L. Position-Sensorless Hybrid Sliding-Mode Control of Electric Vehicles With Brushless DC Motor. IEEE Trans. Veh. Technol. 2021; 70: 421-432.
- [11] Yang B, Yu T, Shu HC, et al. Perturbation observer based fractional-order sliding-mode controller for MPPT of grid-connected PV inverters: Design and real-time implementation, Control Engineering Practice 2018; 79:
- [12] Wu Y; Yu X and Man Z. Terminal sliding mode control design for uncertain dynamic systems. Syst. Control Lett. 2018; 64: 281-287.
- Xinghuo, Y.; Man, Z. Fast terminal sliding-mode control design for nonlinear dynamical systems. IEEE Trans. Circuits Syst. I Fundam. Theory Appl. 2002, 49, 261-264.
- [14] Mu C, Xu W and Sun C. On Switching Manifold Design for Terminal Sliding Mode Control. J. Frankl. Inst. 2016; 353.
- [15] Lu E, Li W, Yang X, et al. Composite Sliding Mode Control of a Permanent Magnet Direct-Driven System For a Mining Scraper Conveyor. IEEE Access 2017; 5:22399-22408.
- [16] Huang, J.; Li, H.; Teng, F.; Liu, D. Fractional order sliding mode controller for the speed control of a permanent magnet synchronous motor. In Proceedings of the 24th Chinese Control and Decision Conference (CCDC), Taiyuan, China, 23–25 May 2012; pp. 1203-1208.
- [17] Bigdeli N and Ziazi HA. Design of fractional robust adaptive intelligent controller for uncertain fractional-order chaotic systems based on active control technique, Nonlinear Dyn.

- [18] Zaihidee FM, Mekhilef S. and Mubin M. Fractional order SMC for speed control of PMSM. In Proceedings of the 6th International Electrical Engineering Congress (iEECON2018), Krabi, Thailand, 7-9 March 2018.
- [19] Huang, J.; Li, H.; Teng, F.; Liu, D. Fractional order sliding mode controller for the speed control of a permanent magnet synchronous motor. In Proceedings of the 24th Chinese Control and Decision Conference (CCDC), Taiyuan, China, 23–25 May 2012; pp. 1203-1208.
- [20] Abdelhamid, D.; Bouden, T.; Boulkroune, A. Design of Fractional-order Sliding Mode Controller (FSMC) for a class of Fractional-order Nonlinear Commensurate Systems using a Particle Swarm Optimization (PSO) Algorithm. J. Control Eng. Appl. Inform. 2014, 16, 46-55.
- [21] Mahmoodabadi MJ and Nemati AR. A novel adaptive genetic algorithm for global optimization of mathematical test functions and real-world problems, Eng. Sci. Tech., Int. J., 2016.
- [22] Laware AR, et al. Evolutionary optimization of sliding mode controller for level control system. ISA Transactions, 2018.
- [23] Mousavian SH and Koofigar HR. Identification-Based Robust Motion Control of an AUV: Optimized by Particle Swarm Optimization Algorithm, J Intell Robot Syst.
- [24] Thanok S and Parnichkun M. Longitudinal control of an intelligent vehicle using particle swarm optimization based sliding mode control, Advanced Robotics 2015; 29(8): 525-543.
- [25] Ibrahim B, Abdelkader H, Amine M, et al. Optimization of Sliding Mode Control for Doubly Fed Induction Generator Systems Using Particle

- Swarm and Grey Wolf Algorithms, Electric Power Components and Systems 2024; 52(10): 1782-1795.
- Soufi Y, et al., Particle swarm optimization based sliding mode control of variable speed wind energy conversion system, International Journal of Hydrogen Energy 2016.
- [27] Chen ZM, Meng WJ, Zhang JG et al. Scheme of Sliding Mode Control based on Modified Particle Swarm Optimization, Systems Engineering -Theory & Practice 2009; 29(5).
- [28] Terfia ES, Mendaci S, Rezgui SE et al. Optimal third-order sliding mode controller for dual star induction motor based on grey wolf optimization algorithm, Heliyon 10 2024; e32669.
- Lindokuhle J. Mpanza and Jimoh O. Pedro, Sliding Mode Control Parameter Tuning Using Ant Colony Optimization for a 2-DOF Hydraulic Servo System, 2016 IEEE International Conference on Automatic Control and Intelligent Systems (I2CACIS), 22 October 2016, Shah Alam, Malaysia.
- [30] Anuja S. Joshi, et al. Cuckoo Search Optimization- A Review. Materials Today: Proceedings 2017; 4: 7262-7269.
- Zamani AA, Tavakoli S and Etedali S. Fractional order PID control design for semi-active control of smart base-isolated structures: A multiobjective cuckoo search approach, ISA Transactions, 2017.
- [32] Cuong-Le T, Hoang-Le M, Khatir S, et al. A novel version of Cuckoo Search Algorithm for solving Optimization problems, Expert Systems with Applications, 2021.